N72-10058

Density and Fluence Dependence of Lithium Cell Damage and Recovery Characteristics

T. J. Faith, Jr.
RCA Astro Electronics Division
Princeton, N. J.

ABSTRACT

Experimental results on lithium-containing solar cells point toward the lithium donor density gradient dN_L/dw as being the crucial parameter in the prediction of cell behavior after irradiation by electrons. Recovery measurements on a large number (180) of oxygen-rich and oxygen-lean lithium cells fabricated by all three manufacturers have confirmed that cell recovery speed is directly proportional to the value of the lithium gradient for electron fluences ranging from 3×10^{13} e/cm^2 to 3×10^{15} e/cm^2. An approximate relationship between the time to half recovery, θ, (at room temperature) the lithium gradient, dN_L/dw, and the 1-MeV electron fluence Φ was derived for oxygen-rich cells:

$$\theta \, dN_L/dw \approx 2.7 \times 10^{12} \Phi^{0.57} \text{ days/cm}^4$$

which holds for the entire range of fluences tested. For oxygen-lean (Centralab and Heliotek) cells the relation

$$\theta \, dN_L/dw \approx 8.5 \times 10^{8} \Phi^{0.61} \text{ days/cm}^4$$

holds up to 1×10^{15} e/cm^2, above which a more rapid increase with fluence occurs, probably due to the greater significance of lithium depletion during irradiation. A similar relationship holds for oxygen-lean Texas Instruments cells, but with a proportionality constant approximately ten times that of the cells from the other manufacturers.

Seventy oxygen-rich (C13) cells with initial performance significantly above a group of commercial 10 Ω-cm n/p cells were recently irradiated to fluences ranging from 3×10^{13} to 3×10^{15} e/cm^2. Through pre-irradiation capacitance measurements (giving dN_L/dw) and pre- and post-irradiation short-circuit current and diffusion length measurements, a relationship was derived between the diffusion length damage constant before recovery, $K_L(O)$, and dN_L/dw and Φ.

$$K_L(O) = 5.3 \times 10^{-18} (dN_L/dw)^{1/2} (1 - 0.063 \log_{10} \Phi)$$

Gradient measurements have also been correlated with lithium diffusion schedules. Results have shown that long diffusion times (≥5 h) with a paint-on source result in large cell-to-cell variations in gradient, probably due to a loss of the lithium source with time. They also indicate that this problem can be overcome either by short diffusion times or by use of an evaporated lithium source.

I. INTRODUCTION

The principal performance parameters characterizing lithium cell behavior in a radiation environment are: (1) the initial (pre-irradiation) performance levels, (2) the rate of cell degradation or damage constant, (3) cell recovery rate versus cell temperature, and (4) final photovoltaic performance after recovery from a given fluence. Under the present contract, experiments on solar cells irradiated by 1-MeV electrons have been designed with the aim of eventually relating the

above performance parameters and the manufacturers' fabrication parameters to a set of physical parameters obtainable through non-destructive measurements on unirradiated cells. This would provide the cell manufacturers with: (1) the optimum set of fabrication parameters for a given cell application, and (2) a set of quality-control tests that can be integrated into the production line.

In earlier work on this contract the dependence of recovery rate on cell temperature was obtained for both oxygen-rich and oxygen-lean lithium cells through measurements of activation energy for diffusion-length recovery (Ref. 1). For a given cell temperature, the recovery rate of short-circuit current in the 10^{14} e/cm^2 fluence range was shown to vary linearly with the lithium density gradient (Ref. 2) for both oxygen-rich and oxygen-lean cells. In recent work: (1) recovery rate versus lithium gradient measurements were extended to cover the fluence range from 3×10^{13} to 3×10^{15} e/cm^2; (2) a relationship between diffusion-length damage constant K_L, lithium gradient dN_L/dw, and 1-MeV electron fluence Φ were obtained through measurements on seventy irradiated cells of lot C13, and (3) pre-irradiation capacitance measurements on one hundred C13 cells established relationship between fabrication parameters (temperature and time of lithium diffusion) and the degree of control of the lithium density gradient, dN_L/dw, near the junction.

II. INITIAL CELL PERFORMANCE

A shipment of one hundred high performance lithium cells fabricated from quartz-crucible silicon (lot C13) were recently received from JPL. They consisted of ten groups (C13A to C13J), ten cells per group, with varying lithium diffusion temperatures and diffusion times. Lithium density gradients were obtained from reverse-bias capacitance measurements (Ref. 3) on all of the C13 cells. Some of the individual groups showed large cell-to-cell variations in gradient. This finding and its relationship to the individual cell groups will be discussed later in the paper; in this section the cells are divided into three batches according to lithium gradient, without distinctions between groups. The three photovoltaic parameters, maximum power, P_{max}; short-circuit current, I_{sc}; and open-circuit voltage, V_{oc}, are plotted in Figs. 1, 2, and 3, respectively. For these figures the cells were divided into batch 1, consisting of 20 cells with gradient ranging from 0.65×10^{18} to 3.3×10^{18} cm^{-4}; batch 2, with 40 cells ranging from 3.3×10^{18} to 9.0×10^{18} cm^{-4}; and batch 3, with 40 cells ranging from 9.0×10^{18} to 1.6×10^{19} cm^{-4}.[1]

The data points appear along the abscissa at the average value of dN_L/dw for the batch and the five ordinates represent (from top to bottom) the highest value, the values exceeded by 20, 50, and 80% of the cells, and the lowest value for the batch. Equivalent values for a batch of 20 commercial 10 Ω-cm N/P cells are shown on the left in each figure. The general trends show the power and short-circuit current to remain approximately constant over the first two batches, then drop with batch 3, while the open-circuit voltage increases monotonically with gradient. The maximum power of all lithium batches exceeds that of the n/p batch, most of this advantage being due to the higher V_{oc} which is due, in turn, to the heavier base doping in the lithium cells.

III. DAMAGE CONSTANT

Seventy of the C13 cells were irradiated with 1 MeV electrons; seventeen cells to a fluence of 3×10^{13} e/cm^2, nine to 1×10^{14} e/cm^2, twenty to 3×10^{14} e/cm^2, eight to 1×10^{15} e/cm^2, and sixteen to 3×10^{15} e/cm^2. The cells were chosen so that seven cells from each group were irradiated, and so that the cells irradiated to 3×10^{13} e/cm^2, 3×10^{14} e/cm^2 and 3×10^{15} e/cm^2 covered the widest possible range of lithium gradients. Room-temperature photovoltaic characteristics under 140 mW/cm^2 tungsten illumination were taken on all cells immediately after irradiation. The cells were then stored at 80°C to recover.

A number of interesting results were obtained from the short-circuit current readings made immediately after irradiation (before recovery). This current is plotted in Fig. 4 versus lithium donor density gradient, dN_L/dw, for the seventy irradiated cells. Within the scatter of the data, the points at each fluence fit well along a straight line, all five lines having approximately the same slope. A best least-squares fit to the equation

$$I_{sc} = I_A - B \log_{10} (10^{-18}\, dN_L/dw) \qquad (1)$$

was calculated for each fluence.

The values of B were found to be 8.4, 8.7, 8.4, 8.5 and 8.9 for $\phi = 3 \times 10^{13}$, 1×10^{14}, 3×10^{14}, 1×10^{15}, and 3×10^{15} e/cm^2, respectively. These equations give a specific relation between the amount of initial damage (before recovery) and the lithium gradient in crucible-grown cells. It is advantageous to describe this damage in terms of a more standard quantity, namely the diffusion-length damage constant before recovery, $K_L(O)$, given by

$$K_L(O)\Phi = \frac{1}{L(O)^2} - \frac{1}{L_0^2} \qquad (2)$$

where L_0 and $L(O)$ are the diffusion lengths in the base region of the cell before irradiation and immediately after irradiation, respectively. To obtain $K_L(O)$, the relationship between I_{sc} and L must be known; Fig. 5 gives such a plot for C13 cells. The data for this figure was generated from simultaneous short-circuit-current and diffusion length[2] measurements (Ref. 4) made on the C13 cells, 30 of which were unirradiated, the other

[1] Batch 1 has the smaller number of cells because of the comparatively small fraction of cells in the low gradient range.

[2] Obtained from measurements using band-gap light that was calibrated with the electron-voltaic method using 15 different lithium and N/P solar cells.

70 being at various stages of recovery after irradiation. The best fit to this data is

$$I_{sc} = 34.4 \log_{10} L \qquad (3)$$

For fluences above 3×10^{13} e/cm^2, $1/L(O)^2 \gg 1/L_0^2$ in Eq. (2) and the latter term can be dropped with less than 10 percent error. This approximation, combining Eqs. (1), (2) and (3), and using B = 8.6 in Eq. (1), gives

$$K_L(O) = \frac{10^{-(1+I_A/17.2)}}{\Phi} \sqrt{\frac{dN_L}{dw}} \qquad (4)$$

which is valid for all of the fluences employed except $\Phi = 3 \times 10^{13}$ e/cm^2. For this lowest fluence $K_L(O)$ was calculated taking L_0 into account. The result, which is shown in Fig. 6, was

$$K_L(O) = 8.5 \times 10^{-19} \sqrt{dN_L/dw} \qquad (5)$$

Equations (4) and (5), together with the appropriate values of I_A listed in Fig. 4, give the fluence dependence of $K_L(O)$, which is plotted in Fig. 7 for $dN_L/dw = 10^{18}$ cm^{-4}. Figure 7 shows a logarithmic dependence on fluence described (for $dN_L/dw = 10^{18}$ cm^{-4}) by

$$K_L(O) = 5.3 \times 10^{-9}(1 - 0.063 \log_{10} \Phi) \qquad (6)$$

Inserting the lithium gradient dependence, the expression for K_L as a function of Φ and dN_L/dw is given by

$$K_L(O) =$$

$$5.3 \times 10^{-18} (dN_L/dw)^{1/2} (1 - 0.063 \log_{10} \Phi) \qquad (7)$$

The applicability of this relationship to other crucible cells was tested using the post-irradiation data on thirteen previously irradiated cells from lot H3A. These H3A cells covered a wide range of gradients: $3 \times 10^{17} \leq dN_L/dw \leq 1.3 \times 10^{19}$ cm^{-4}; they were irradiated to a fluence of 3×10^{14} e/cm^2. Figure 8 shows $K_L(O)$ plotted against dN_L/dw for these cells. The square-root dependence on gradient is evident, the best least-squares fit being obtained with the relationship

$$K_L(O) = 4.4 \times 10^{-19} (dN_L/dw)^{1/2} \qquad (8)$$

This is within 10% of the value of 4.8×10^{-19} $(dN_L/dw)^{1/2}$ obtained for the C13 cells, as can be seen in Fig. 7, where the H3A data point is shown together with the C13 data.

The C13 cells are now recovering at 80°C. At completion of short-circuit current recovery, the effective damage constant, $K_L(R)$, after cell recovery can be computed from

$$K_L(R)\Phi = \frac{1}{L(R)^2} - \frac{1}{L_0^2} \qquad (9)$$

where L(R) is the diffusion length after recovery. There is a large uncertainty in $K_L(R)$ for low fluences since $I(R) \sim I_0$. Results at 3×10^{13} e/cm^2 show a very large scatter, $K_L(R)$ ranging from 0.5×10^{-10} to 2.0×10^{-10} e^{-1}. The results at 1×10^{-14} e/cm^2 are more coherent and show a slight increase with lithium gradient, $K_L(R)$ ranging from 1.0×10^{-10} to 1.6×10^{-10} e^{-1} for gradients ranging from 4×10^{18} to 1.6×10^{19} cm^{-4}.

IV. RECOVERY CHARACTERISTICS

Prior to the tests on the C13 cells, a large number of previously unirradiated oxygen-lean cells from past shipments were gathered and irradiated to fluences ranging from 3×10^{13} e/cm^2 to 3×10^{15} e/cm^2. Cells from Texas Instruments, Heliotek and Centralab[3] of both Lopex[4] and float-zone silicon were represented. They included a wide range of diffusion schedules and initial performance levels. After irradiation, short-circuit current was measured as a function of time on all of the cells. The purpose of the experiment was to test the validity of the previously observed (Ref. 2) linear relationship between recovery speed and lithium density gradient for a large batch of cells covering the widest possible range of lithium gradients and a wide range of fluences.

A typical short-circuit current versus time curve during recovery is shown in Fig. 9. The time to half recovery, θ, defined by

$$\frac{I(R) - I(\theta)}{I(R) - I(O)} = 0.5 \qquad (10)$$

where I(R) is the short-circuit current at peak recovery, provides the most well-defined index of (inverse) recovery rate. For the cell in Fig. 9, θ = 55 min (or 0.038 days). The values of θ for the Centralab and Heliotek cells are plotted against lithium density gradient in Fig. 10 for four fluences ranging from 3×10^{13} to 3×10^{15} e/cm^2. Included are all the cells tested from these manufacturers except those of lots C4 and C5 and those with lithium gradients greater than 10^{20} cm^{-4}. The points on these logarithmic plots

[3]Lots T3, T4, T5, T6, T7, T9, T10, H5, H7, H1A, H5A, H7A, H (NASA-furnished in 1967), C4, C5, C8F, C10C, C10F, and C11C were represented.

[4]Trademark of Texas Instruments Corp.

fit remarkably well along straight lines with minus one slope, confirming the linear relationship between recovery speed and lithium gradient. The $\theta\ dN_L/dw$ products (averaged over the cells at each fluence) are: 1.7×10^{17} days/cm^4 for 3×10^{13} e/cm^2; 3.4×10^{17} days/cm^4 for 1×10^{14} e/cm^2; 7.2×10^{17} days/cm^4 for 3×10^{14} e/cm^2, and 6.8×10^{18} days/cm^4 for 3×10^{15} e/cm^2. There are two cell lots that do not follow these curves, lots C4 and C5, which recover at a faster rate than the curves predict. However, these two lots had already been identified as mavericks in previous work (Ref. 2), having been shown to suffer open-circuit voltage instability due to a decrease in lithium gradient with time. In addition, cells with gradients greater than 10^{20} cm^{-4} (C10C and C10F cells) recovered more slowly at low fluence than predicted by the curves. A feasible explanation for this is that the gradient in these cells is not a good index of the average lithium density near the junction. The capacitance measurements on these high gradient cells give evidence of this in the form of a leveling off of the lithium density; i.e., a decrease in gradient, at distances of less than 1 μm from the junction.

Curves of θ versus dN_L/dw for oxygen-rich crucible cells are shown in the upper portion of Fig. 10. The data are drawn from previous results on cells that recovered at room temperature, 60°C, or 80°C. (In the latter two cases equivalent recovery time at room temperature was calculated using the activation energy previously obtained (Ref. 1) for crucible cell recovery.) At 1×10^{14} e/cm^2 and 3×10^{14} e/cm^2 the separation between the oxygen-lean (FZ and L) curve and the crucible curve is ≈700, which is approximately the ratio of the room-temperature lithium diffusion constant in oxygen-lean silicon to that in oxygen-rich silicon (Ref. 5). At the highest fluence, 3×10^{15} e/cm^2, the separation is only ≈250. This suggests that lithium is lost more rapidly in defect formation in oxygen-lean cells than in oxygen-rich cells, supporting previous carrier removal observations (Ref. 1) in bulk-sample measurements.

A puzzling anomaly was observed in the case of the oxygen-lean T cells. While the constancy of the $\theta\ dN_L/dw$ product was satisfied by these cells at each fluence as shown in Fig. 11, the products were approximately an order of magnitude higher than the equivalent products for the Centralab and Heliotek cells. This can be seen by comparing the products in Fig. 11 with those of Fig. 10. This discrepancy is not understood at present. One of the main differences between the manufacturers is that the TI cells have used an evaporated lithium source whereas all of the oxygen-lean C and H cells tested to date have used a paint-on source. It would seem likely that a difference in silicon type would cause differences in recovery rate. This would be particularly feasible for Lopex versus float-zone recovery since the oxygen-content is generally higher in Lopex silicon. However, as was shown in Fig. 10, the same recovery rate applies for both Lopex and float-zone C and H cells. Dislocation counts are now being made on some of the cells in an effort to confirm the silicon types employed.

The approximate linear dependence of recovery speed on lithium gradient at all the fluences tested enables prediction of the recovery speed of any lithium cell with lithium gradient between 10^{17} and 10^{20} cm^{-4} in this fluence range. This is illustrated in Fig. 12, which gives plots of the $\theta\ dN_L/dw$ products of all the cells tested versus 1-MeV electron fluence.

Below 10^{15} e/cm^2 this product increases gradually with fluence in all types of cells. In oxygen-lean cells there is a more pronounced dependence on fluence above 10^{15} e/cm^2. In the oxygen-rich cells the relation

$$\theta\ dN_L/dw = 2.7 \times 10^{12} \Phi^{0.57}\ \text{days/cm}^4 \qquad (11)$$

provides a good approximation of cell recovery speed over the entire range of fluences.

V. LITHIUM DIFFUSION SCHEDULE AND DENSITY CONTROL

From the above and previous results, it is evident that many of the characteristics of lithium cells under electron irradiation can be predicted through knowledge of the lithium density gradient, dN_L/dw. Consequently, it is desirable to find relationships between this parameter and the fabrication parameters of the cell manufacturers. This has been accomplished for cell lots C13 (100 cells) and H3A (15 cells). Lot C13 consists of 10 groups of 10 cells, comprising nine different lithium diffusion schedules with diffusion temperatures ranging from 330°C to 370°C and diffusion times from 3 to 7 h. The lithium source was a lithium-in-oil suspension painted on the back surface of the cell. Figure 13 gives the distribution of lithium gradients measured for the cells in each of the 10 cell groups. There are five separate ordinates, each running from 1 to 10. The value of the ordinate at a given lithium gradient indicates the number of cells of that particular group with a lithium gradient greater than the value of the abscissa. A pair of cell groups shares each ordinate, since two groups were diffused at each lithium diffusion temperature. Each group is identified by a letter followed by a number in parentheses which gives the lithium diffusion time in hours.

Several important factors are brought out in Fig. 13: (1) for a given diffusion temperature, the shorter diffusion time gives a narrower gradient distribution; i.e., better gradient control; (2) the gradient distribution for the shorter diffusion time is always situated near the upper limit of that for the longer diffusion time; (3) at the highest diffusion temperature, even the short time diffusion shows a rather broad distribution; and (4) the average gradient (for short diffusion times) increases with diffusion temperature. Items (1), (2), and (3) indicate that as the diffusion time increases the lithium reservoir is somehow lost to the cell, either through lithium depletion or through interruption of the lithium-silicon interface. Therefore, for lithium introduction by the paint-on technique, the shortest practical diffusion time should be used.

A previously received cell lot, H3A, consisted of 15 quartz-crucible cells diffused with lithium for 8 h at 325°C. Ten of the cells used a paint-on source; the other five, an evaporated lithium

source. The cell distribution versus lithium gradient is shown in Fig. 14. The cells using the paint-on source have a very broad distribution similar to those of the C13 cells using long diffusion times. The cells using an evaporated source, however, have a narrow distribution at the high end of the gradient scale. This supports the hypothesis of loss of the lithium source in the paint-on cells and also indicates that an evaporated source may provide the solution to this problem.

VI. CONCLUSIONS

Previous work has shown the lithium density gradient, dN_L/dw, obtained from non-destructive capacitance measurements, to be a convenient and useful way to characterize the lithium density in a lithium cell by a single parameter. The present work has investigated the relationship between this physical parameter and the performance and recovery parameters of the lithium cell. Results show that knowledge of the lithium gradient enables the prediction of recovery speed for both oxygen-rich and oxygen-lean cells within a factor of approximately 2 for 1 MeV-electron fluences from 3×10^{13} to 3×10^{15} e/cm^2.

A relationship between the diffusion-length damage constant immediately after irradiation (before recovery) $K_L(O)$, the lithium gradient, dN_L/dw, and the electron fluence, Φ, has been obtained for C13 crucible cells:

$$K_L(O) = 5.3 \times 10^{-18} (dN_L/dw)^{1/2} (1 - 0.063 \log_{10} \Phi)$$

A check on previous post-irradiation data shows that this relationship also holds for H3A cells irradiated to 3×10^{14} e/cm^2. One additional relationship, that between the damage constant after recovery $K_L(R)$, dN_L/dw, and ϕ, is required to complete the description of cell dynamics under electron irradiation. The C13 cells are now recovering, and this will be investigated upon completion of recovery.

These relations make it possible, in principle, to predict cell behavior in an electron environment using a simple non-destructive capacitance measurement. It is evident that a similar approach to predicting cell behavior under heavy particle irradiation should also be examined.

Gradient measurements have also been correlated with lithium diffusion schedules. Results have shown that long diffusion time ($\gtrsim$5 h) with a paint-on source result in large cell-to-cell variations in gradient, probably due to a loss of the lithium source with time. The results also indicate that this problem can be overcome either by short diffusion times or by use of an evaporated lithium source.

REFERENCES

1. Brucker, G., et al., Fourth Quarterly Report, RCA under JPL Contract No. 952555, July 10, 1970.

2. Faith, T., Brucker, G., and Holmes-Siedle, A., Sixth Quarterly Report, JPL Contract No. 952555. Prepared by RCA and issued Jan. 10, 1971; see also Faith, T., Corra, J. P., and Holmes-Siedle, A., Conference Record of the Eighth Photovoltaic Spec. Conf., IEEE Catalog No. 70C 32 ED, p. 247, 1970.

3. Hilibrand, J., and Gold, R. D., RCA Rev. Vol. 21, p. 245, 1960.

4. Rosenzweig, W., Bell Sys. Tech. J., Vol. 41, p. 1573, 1960.

5. Pell, E. M., J. Appl. Phys. Vol. 31, p. 291, 1960; Vol. 32, p. 6, 1961; and Phys. Rev. Vol. 119, p. 1222, 1960.

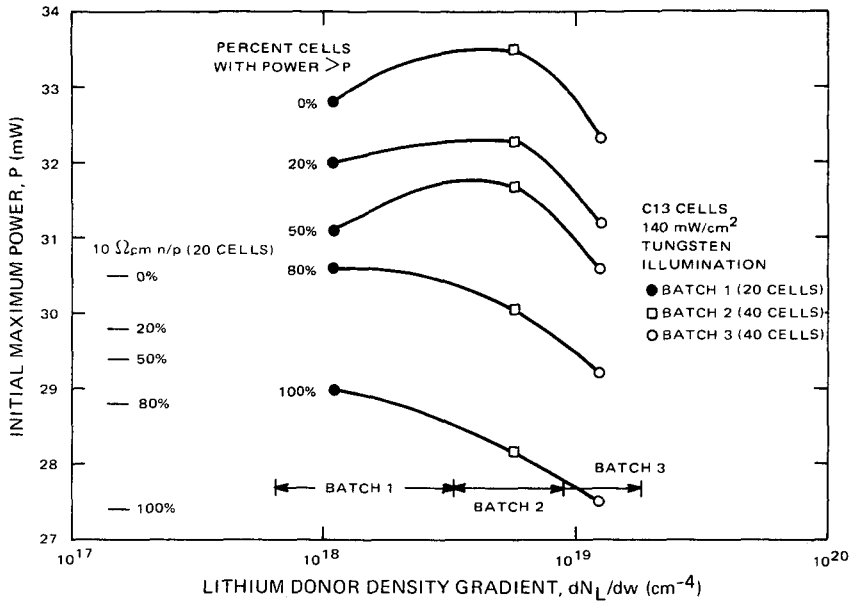

Fig. 1. Initial maximum power distributions for C13 quartz-crucible lithium cells versus lithium donor density gradients with comparisons of 10 Ω-cm commercial N/P cells

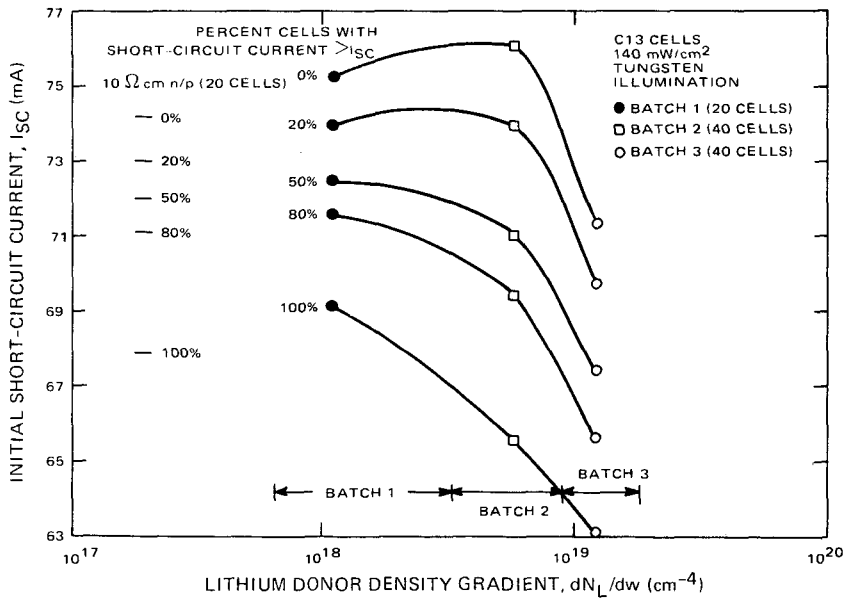

Fig. 2. Initial short-circuit current distributions for C13 quartz-crucible lithium cells versus lithium donor density gradients with comparisons of 10 Ω-cm commercial N/P cells

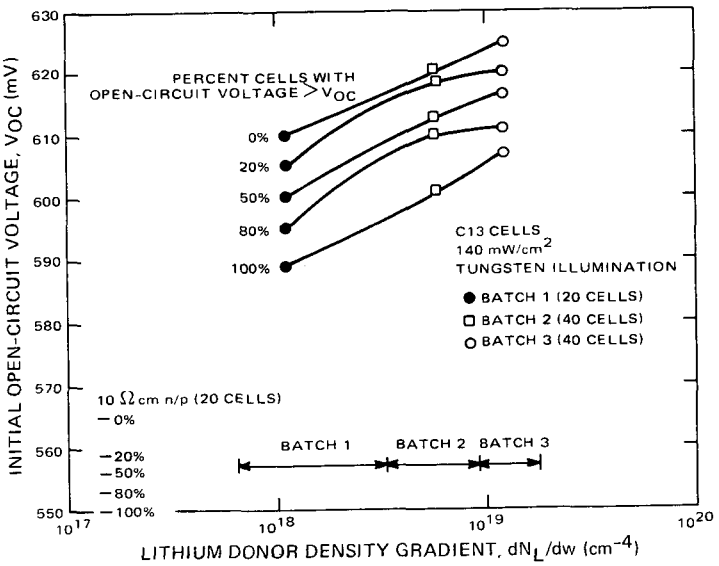

Fig. 3. Initial open-circuit voltage distribution for C13 quartz-crucible lithium cells versus lithium donor density gradients with comparisons of 10 Ω-cm commercial N/P cells

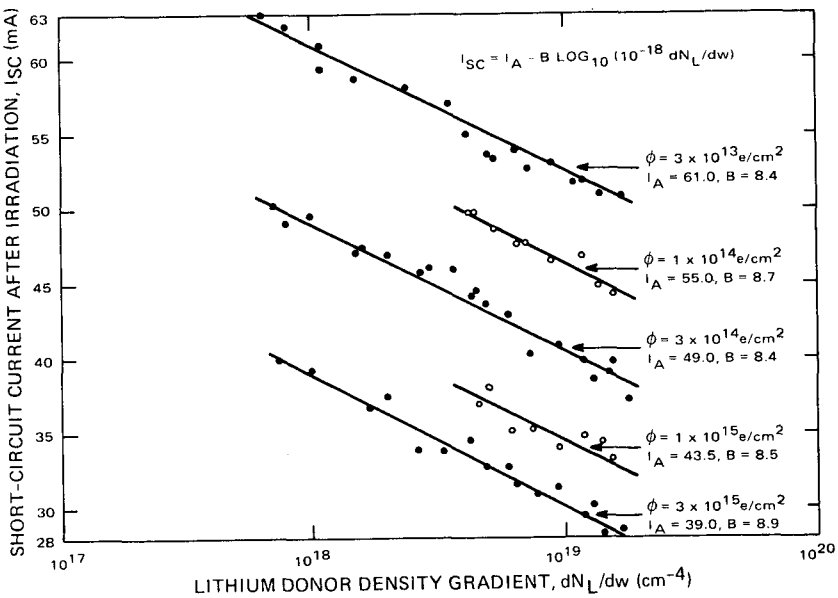

Fig. 4. Short-circuit current immediately after irradiation versus lithium density gradient for seventy C13 cells irradiated by 1-MeV electrons to fluences ranging from 3×10^{13} e/cm^2 to 3×10^{15} e/cm^2

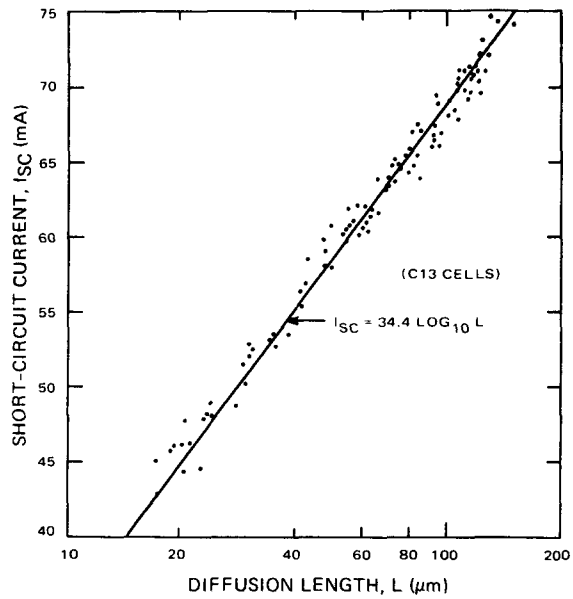

Fig. 5. Short-circuit current versus diffusion length for 100 crucible C13 cells (30 cells unirradiated, 70 cells at various stages of recovery after irradiation)

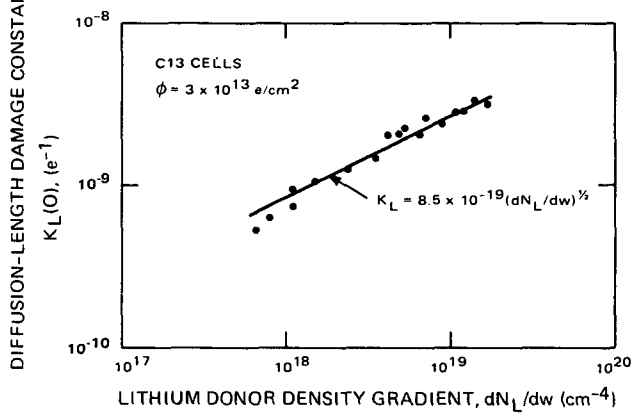

Fig. 6. Diffusion-length damage constant immediately after irradiation (before recovery) versus lithium gradient for seventeen C13 cells irradiated to a fluence of 3×10^{13} e/cm^2

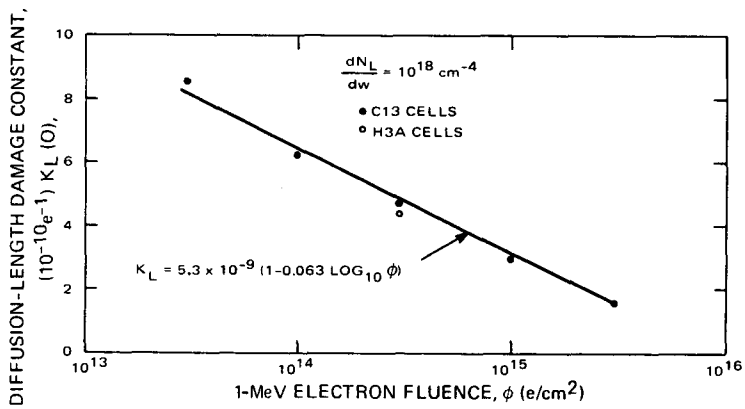

Fig. 7. Diffusion-length damage constant immediately after irradiation (at $dN_L/dw = 10^{18}$ cm^{-4}) versus 1-MeV electron fluence for C13 and H3A cells

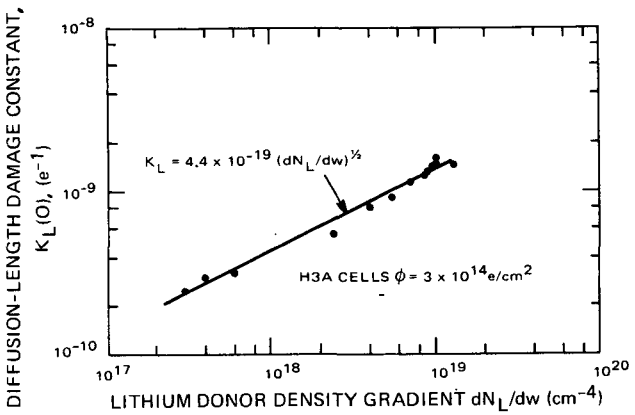

Fig. 8. Diffusion-length damage constant immediately after irradiation versus lithium gradient for H3A cells irradiated to a fluence of 3×10^{14} e/cm^2

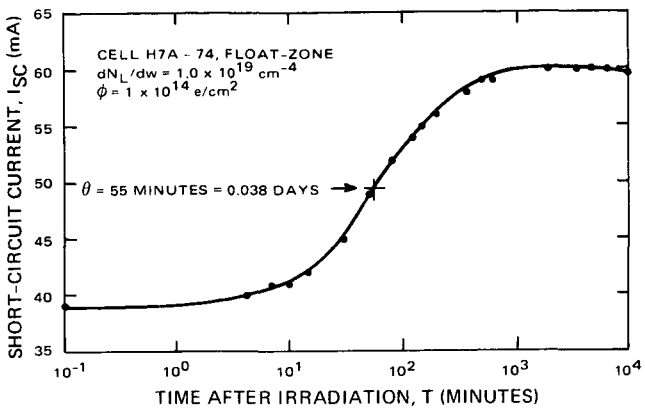

Fig. 9. Typical short-circuit current recovery curve illustrating the index of cell recovery rate θ used in subsequent illustrations

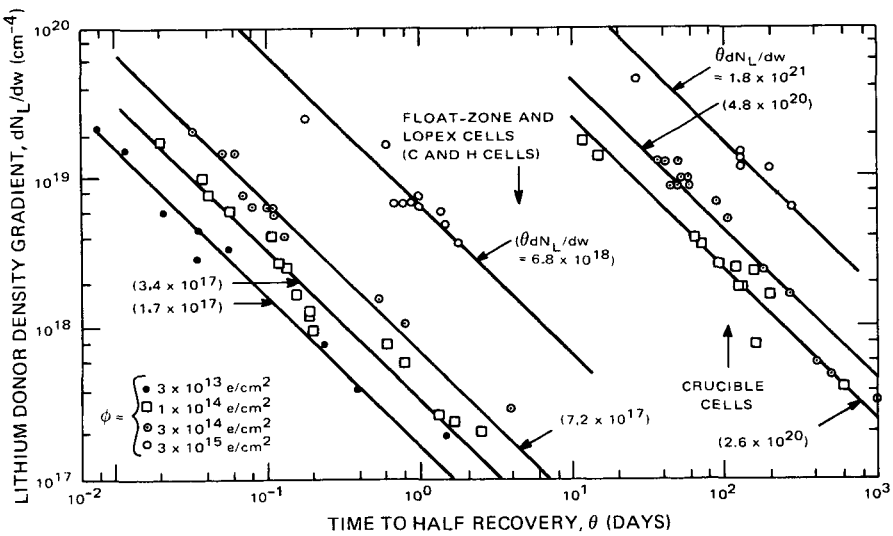

Fig. 10. Time to half recovery at room temperature versus lithium gradient for oxygen-rich cells and for Centralab and Heliotek oxygen-lean cells irradiated to fluences ranging from 3×10^{13} to 3×10^{15} e/cm^2

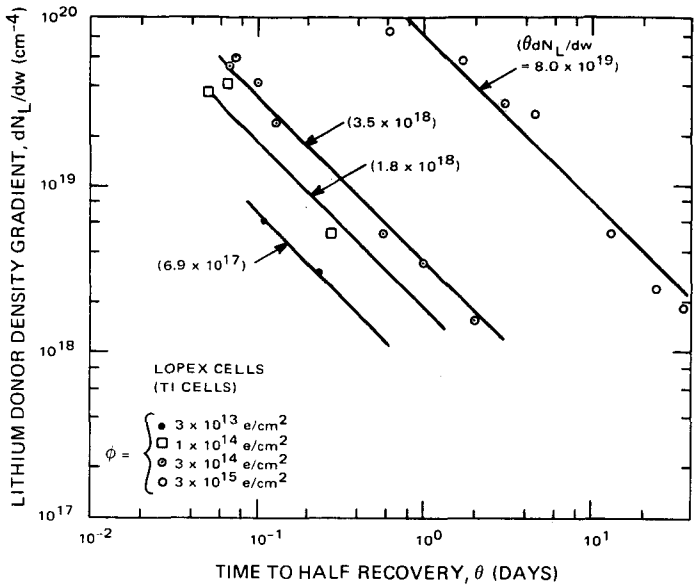

Fig. 11. Time to half recovery at room temperature versus lithium gradient for oxygen-lean Texas Instruments cells irradiated to fluences ranging from 3×10^{13} to 3×10^{15} e/cm^2

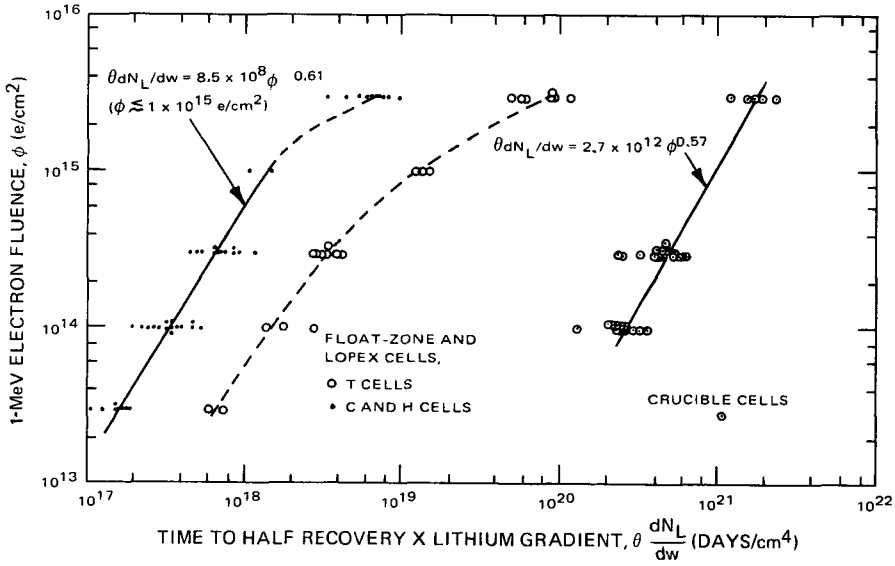

Fig. 12. Product of time to half recovery and lithium gradient, θ dN_L/dw plotted versus 1-MeV electron fluence for oxygen-rich and oxygen-lean lithium cells

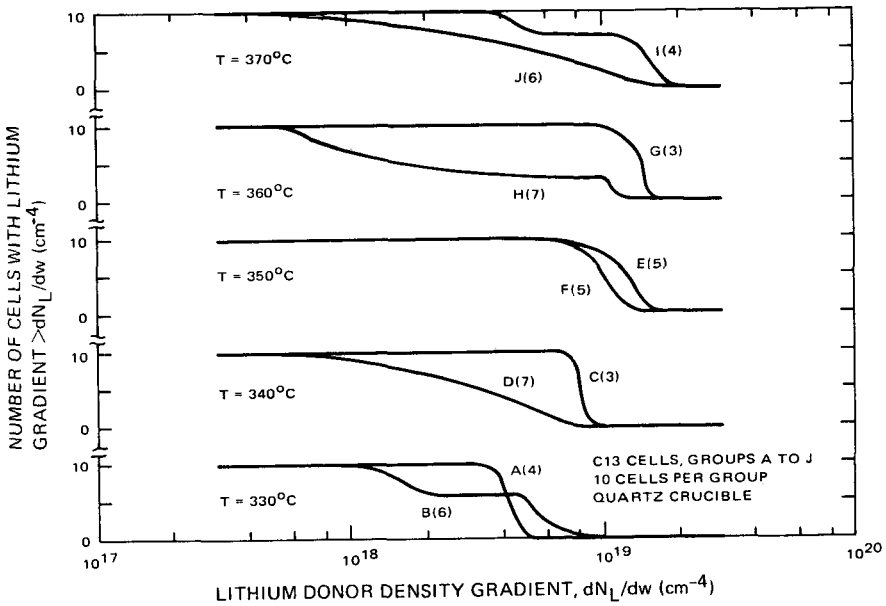

Fig. 13. Distribution of cells versus lithium gradient for the ten different cell groups within Lot C13. Numbers in parentheses indicate duration of lithium diffusion in hours; T = diffusion temperature

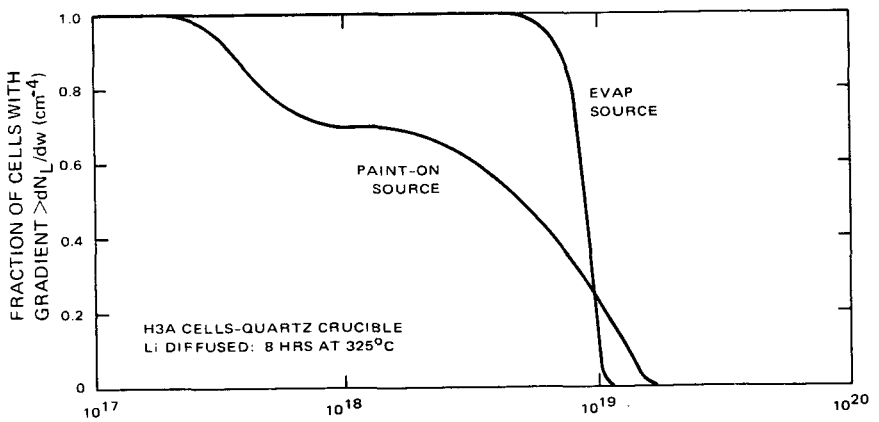

Fig. 14. Distribution of cells versus lithium gradient for H3A cells using two different lithium sources, paint-on and evaporated